

Estimation and Evaluation of Tissue Inhomogeneity Effect on Dose Distribution for High Dose Rate Iridium 192 Source Using Monte Carlo Simulation and Film Dosimetry

Akbar Adelnia¹ and Daryoush Fatehi^{2*}

¹Department of Medical Physics, Faculty of Medicine, Tarbiat Modares University, Tehran, Iran

²Department of Medical Physics, Faculty of Medicine, Shahrekord University of Medical Sciences, Shahrekord, Iran

Abstract

The aim of this work was to present a theoretical analysis of how phantom dimensions and tissue heterogeneities in interstitial brachytherapy affect on dose distributions. This work was carried out using Gafchromic film measurement and Monte Carlo simulation for ¹⁹²Ir source. Results show that treatment planning systems (TPS) which consider the patient geometry as homogeneous medium, lead to a dose underestimation up to 8.2% for lung and an overestimation up to 9% for bone. These values depend on the thickness and distance from the source. Thus, TPSs currently in use for clinical brachytherapy cannot consider the effect of tissue heterogeneity on dose distribution.

Keywords: Inhomogeneity; Iridium 192; Monte Carlo simulation; Film dosimetry

Introduction

For cancer treatment, many techniques are available. Brachytherapy is one of these methods that play an important role in the treatment of cancers. In this way, small encapsulated radioactive sources were used inside or at a short distance from the target volume for radiation of malignant tumors [1-3]. The main aim of brachytherapy is to deliver lethal dose to tumour cells while minimum dose to healthy tissue surrounded the tumors and spare them as much as possible due to the effect of inverse square law on the dose distribution around the sources [1,2]. Dose calculation algorithms of treatment planning systems (TPS) that are commercially available for clinical brachytherapy rely on pre calculated Monte Carlo (MC) simulation. This results in homogeneous water mathematical phantoms that are either unbounded or most commonly spherical with a radius of 15 cm. These systems assume that full scatter exists in clinical applications [4-7]. Thus, the effects of the presence of heterogeneities and the variable dimensions of patient-specific anatomy in TPSs are ignored and TPSs allocate equally attenuation coefficient to the entire patient's body tissues [6,8,9]. Also, the radioactive sources that generally are utilized for brachytherapy such as ¹²⁵I, ¹⁰³Pd, ¹³⁷Cs and ¹⁹²Ir emit lower energy photons than those used in external radiotherapy. This cause more importance of inhomogeneity effect in brachytherapy treatments [10,11]. One of the most important moot points in brachytherapy, as external radiotherapy method, is dose distribution in patient's body. The successful and effective treatment with lesser side effect for healthy tissue strongly depends on dose distribution in tumour and surrounded healthy tissues. Hence, accuracy of dose calculation in brachytherapy is a high-priority and effective factor to patient treatment that strongly depends on the mass effective attenuations coefficients used in TPS algorithm [3,12]. On the other hand, dose and dose rate distribution are pertained to probability of photoelectric and Compton interactions of the photons [10]. This probability in homogenous medium depends on photon energies, atomic number, density and electron density. Energy increasing leads to decrease of possibility of photoelectric and increment of Compton interaction. The accuracy in dose delivery is very important for treatment and appearance of side effects, however; patient's inhomogeneities cause to change isodose curves related to homogeneous situation that TPSs assume [13]. This subject is more important especially at organs at risk. Since the photoelectric have

heavy contribution in absorbed dose, this phenomenon is particularly important, because the probability of photoelectric interaction strongly depends on the effective atomic number of the involved materials. The current dosimetric formulism for dose prediction in brachytherapy (based on primarily measured TLD data) is derived from the American Association of Physicists in Medicine (AAPM) Task Group No.43 (TG-43) reports [4,14] which assume a homogenous medium:

$$\dot{D}(r, \theta) = S_k \cdot \Lambda \frac{G_L(r, \theta)}{G_L(r_0, \theta_0)} \cdot g(r) \cdot F(r, \theta) \quad (1)$$

where S_k is air Kerma strength, Λ is dose rate constant, G_L is geometric function, $g(r)$ is radial dose function and $F(r, \theta)$ is anisotropic function. This formulism also assumed that patient body tissue in and around the implant region is an unbounded homogeneous medium water equivalent and mass energy absorption coefficient as well as dose distributions curves are functions of this information [4,10,15,16]; while, human body is not a homogenous medium and has been formed of different layers of fat, muscle, bone, etc. Each of them has a different density and atomic number. These differences lead to different attenuation coefficient for defined source energy. These heterogeneities complicate the predication of dose distribution. In the present article, we have investigated the effect of radiobiological interest tissue heterogeneities such as lung and bone inside the homogeneous medium for ¹⁹²Ir HDR brachytherapy source using Monte Carlo simulation (MCNP4c) and EBT film dosimetry in an inhomogeneous phantom. The dosimetric data obtained in this work were compared with those from Flexitron[®]-Nucletron treatment planning system (Flexitron 40 channel, Nucletron V 2.6, The Netherlands) and other published work [17]. Purpose of the study was to show a theoretical analysis of how phantom dimensions

***Corresponding author:** Daryoush Fatehi, Department of Medical Physics, Faculty of Medicine, Shahrekord University of Medical Sciences, PO Box 88155-571, Shahrekord, Iran, Tel: 983833335652; Fax: 983833334911; E-mail: d.fatehi@gmail.com

Received September 22, 2016; **Accepted** October 13, 2016; **Published** October 30, 2016

Citation: Adelnia A, Fatehi D (2016) Estimation and Evaluation of Tissue Inhomogeneity Effect on Dose Distribution for High Dose Rate Iridium 192 Source Using Monte Carlo Simulation and Film Dosimetry. J Nucl Med Radiat Ther 7: 312. doi: [10.4172/2155-9619.1000312](https://doi.org/10.4172/2155-9619.1000312)

Copyright: © 2016 Adelnia A, et al. This is an open-access article distributed under the terms of the Creative Commons Attribution License, which permits unrestricted use, distribution, and reproduction in any medium, provided the original author and source are credited.

and tissue heterogeneities affect on dose distribution in interstitial brachytherapy.

Material and Method

Source modeling

Flexi source model source geometry was simulated as carefully as possible, based on the information presented by the manufacture. Source geometry models include, source encapsulation, internal source geometry, distribution of radioactivity within the source, and the stainless-steel cable welded end to the sources for utilize in remote after-loading systems [18]. The simulated source consists of about 30% ^{192}Ir and 70% ^{103}Pt with 21.704 g/cm^3 density active cylinders encased in a palatine. It was presumed that the radioactive material is uniformly distributed within the ^{192}Ir active core. The source has a 5 mm physical length and 1.1 mm outer diameter including a 0.6 mm core diameter and 0.35 mm active length. ^{192}Ir source is an orthovoltage energy photon emitter with mean energy of 380 keV. A more detailed description of the source was given by the manufacture certification. Unlike the previous work that the effect of rounded tip source simplification on the results was assumed to be minimal i.e., less than the statistical uncertainty of the MC calculations, simulation of the rounded tip source was exactly preformed [19]. The simulated source is illustrated in Figure 1.

Monte Carlo simulation

The use of MC method for simulation and analysis has become a well-established standard in the radiation sciences. There are commercially available various versions of MC codes. We employed the MCNP 4C version, which was released in 1999 and has a prominent capability of geometric modeling and calculating dose distribution within the human body. This code uses a three-dimensional (3D) geometry and transports

neutron, photon, and electrons in the energy range from 1 keV to 1 GeV for simulation [20-23]. Low energy phenomena, such as characteristic X-ray and Auger electrons, are accurately modeled. Moreover, in this study electron transports were simulated and deposited dose per unit volume was calculated. By dividing each single mesh voxel to its corresponding mass density, the deposited energy per unit volume was transformed to the deposited energy per unit mass. MCNP4c utilizes the RSICC package DLC-200/MCNPDATA cross section library, because the DLC-200 library is fully justifiable for the dosimetry of ^{192}Ir source [24]. However, based on the previous works for the ^{192}Ir energies, MC dosimetry results are not very sensitive to the details of the cross section library used in the simulation [17,24]. Two separate simulations were performed in this work. Firstly, a single source was simulated in the center of the homogeneous tissue equivalent phantom taking into account the exact geometry and materials of the ^{192}Ir HDR as mentioned previously. Secondly, the simulation was repeated with replacing lung and bone tissue layers (with dimension of $3\text{ cm} \times 3\text{ cm}$) into the water equivalent phantom (with dimension of $30\text{ cm} \times 30\text{ cm} \times 30\text{ cm}$). The latter simulation has been performed to compare MC with resemble TPS calculations which assume patient body like a homogeneous water phantom irrespective of the patient geometry and heterogeneities there in. The photon and electron simulation energy cut off were set to 5 keV and 10 keV, respectively. In order to express the results in terms of the TG-43 formalism (used by the TPS), a separate MC run was performed which calculates the air kerma strength per unit contained activity (SK/ Λ) in terms of UBq^{-1} . The classic design of the micro S electron ^{192}Ir HDR was simulated in an infinite vacuum space and the air kerma per initial photon was calculated in an air cell situated at 100 cm along the transverse axis of the source [17]. For the ^{192}Ir energies, electronic disequilibrium does not affect on the absorbed dose beyond the first

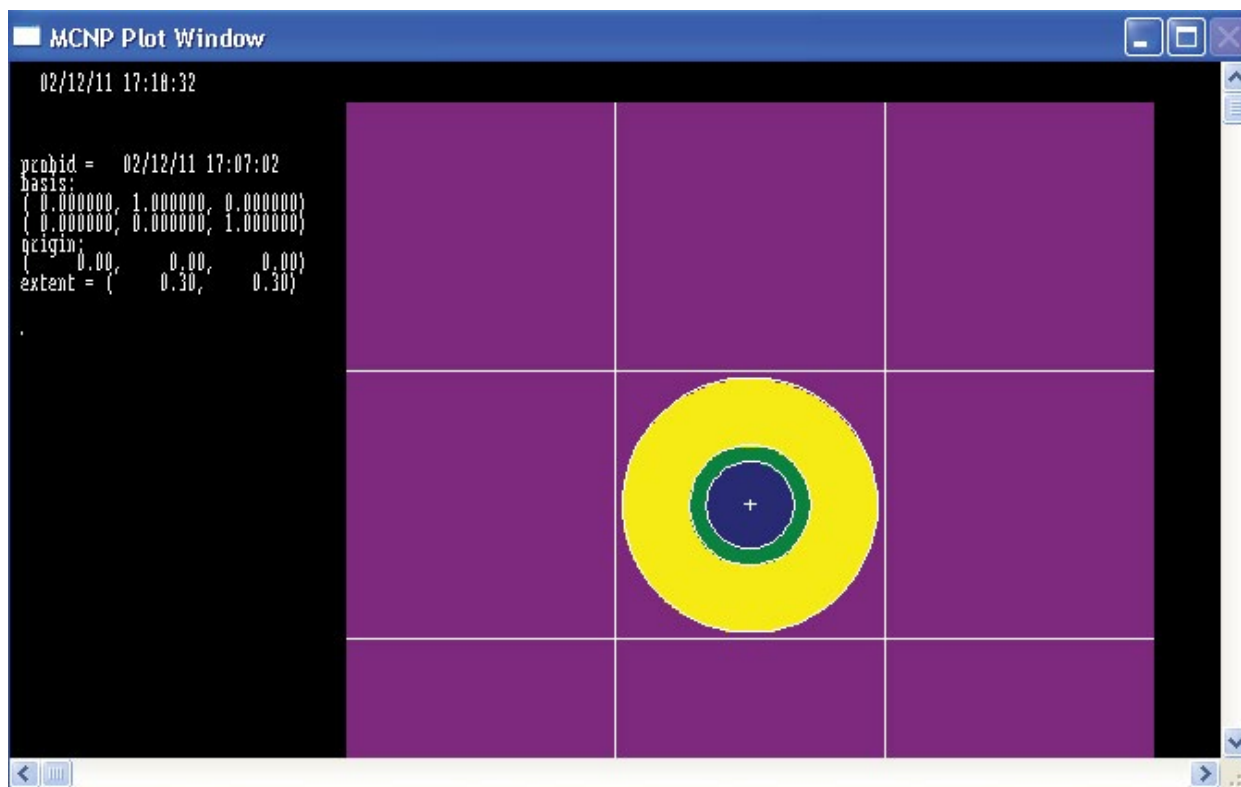


Figure 1: Diagram showing simulated Ir source by Monte Carlo (MCNP4c).

voxel from the surface of the source and the first voxel in the lung-bone interface of the water lung as well as water-bone interface in the phantom [17,24]. The 3D rectangular lattice was extended from -15 cm to 15 cm along the x-, y- and z-axes in relation to the central source dwell position. The voxel size of the 3D lattice was 0.2 cm × 0.2 cm × 0.2 cm along the x-, y- and z-axes so that it is equal to the TPS dose grid resolution. Correspondingly, the *F8 Tally was used in MCNP4c simulations which calculates the energy deposition averaged over a scoring voxel. Although care was taken during the lattice definition in order that lattice cells do not spread over the regions of different material; this was not feasible for the case of the catheter voxels, due to its cylindrical shape. Therefore, dose results at a few voxels lying on the periphery of the stated organs are unphysical and should not be considered in the discussion of the paper [17]. The number of initial photon histories was set to 5×10^7 and 5×10^8 for homogeneous and inhomogeneous phantom geometries, respectively. Simulation for each case on a Pentium IV 2.5 GHz equivalent PC takes about 157 h. In all simulations, relative statistical uncertainty of less than 1% was achieved.

Film dosimetry

Radio chromic film has been used as one of the beneficial dosimeters in the areas of high dose gradient, especially near the brachytherapy sources, where spatial resolution is essential [25-27]. Radio chromic film uses radiochemical process to impart a change in the optical absorbance of the film for specific wavelengths of light. It is almost tissue equivalent and energy independent. High spatial resolution, tissue equivalence, not sensitive to room light and no chemical processing are the main advantages of radio chromic films. The film approximately has not color before irradiation and turns into blue upon exposure to ionizing irradiation and does not require post-irradiation processing [16]. Radio chromic film should be calibrated using a large well characterized uniform radiation field. Film should be placed on the central portion of a large phantom [28,29]. The characteristics of the calibration beam should be determined by some other dosimeters such as ionization chamber [29]. The EBT radio chromic film was used in this study. The geometrical structure and the dosimetric characteristics of these films have been presented in the literatures [30-32]. The film is irradiated by Cobalt machine and an Iridium source at different dose ranges from 0.5 Gy to 8 Gy (with 50 cGy interval). Then, net pixel values of an exposed film were derived from that of an unexposed film. No significant difference was seen between Cobalt and Iridium calibration result. The pixel values were measured using the scanner (Microtek International In, USA, 9800 XL). The relationship between absorbed dose and film response should be determined. This relationship can be plotted as a curve, often known as a calibration curve (Figure 2). The slope of the calibration curve decreases as dose increases. The calibration curve can provide information for conversion of film response to absorbed dose and vice versa. Calibration curve for EBT Gafchromic films were shown in Figure 2. It can be seen that the film response is nonlinear. The data were fit with a fourth-order polynomial. Hence, the following equation was used to convert the data on the experimental films from net pixel value (x) to dose (y):

$$y = -8E-07 \times x^4 + 0.0013 \times x^3 - 0.8853 \times x^2 + 281.55x + 1325.6 \quad (R^2 = 0.9976) \quad (2)$$

The relationship between dose and film response can also be tabulated. Figure 3 shows the films that were used for calibration process. In this work for dosimetry in homogeneous medium the films were located between Perspex slabs against the source catheter, parallel

with the transverse axis. The source-to-film distance was determined by slab thickness at various distances. The effects of heterogeneity and phantom dimension on dose distribution were considered with placing films inter of inhomogeneous layers of cork, as lung; and Teflon, as bone. The scanning system (Microtek International In, USA, 9800 XL) was used for reading out the response of the film (Figure 3). All films were scanned 48 h after exposure using a resolution of 127 mm. A region of interest inside the cut edges of the film was selected to exclude any damage caused by cutting the film and the averaged pixel value of the region was measured using the MATLAB R2012a software. The films were stored and scanned in a laboratory that is consistently maintained near ~22°C. Exposure of the films to fluorescent lighting was kept to minimum during handling.

Result

Phantom validation

TPS dosimetry calculations are based on pre-calculated MC dosimetry data acquired with the ¹⁹²Ir source centred in specific phantom geometries. TPS cannot account any changes in scatter conditions imposed by phantom geometry condition and source dwell positions at different distances in phantom boundary while that is possible in the MC simulation [20-23]. Currently utilized commercial TPS ignores not only the effect of tissue heterogeneity within the patient, but also it denies the effect of the finite patient volume. It calculates dose in either an unbounded or most commonly a 15 cm radius spherical homogeneous water phantom [4,32].

To evaluate the validity of MC simulation, the deposited energy was determined in a simulated spherical, 15 cm radius water equivalent phantom (Figure 4) with a single ¹⁹²Ir source centred in the phantom as well as situated eccentrically at various distances. Using 5×10^8 photon histories in MC simulation, resulting in statistical uncertainty of the dose distribution of roughly 0.5% near the source and 1% for distances

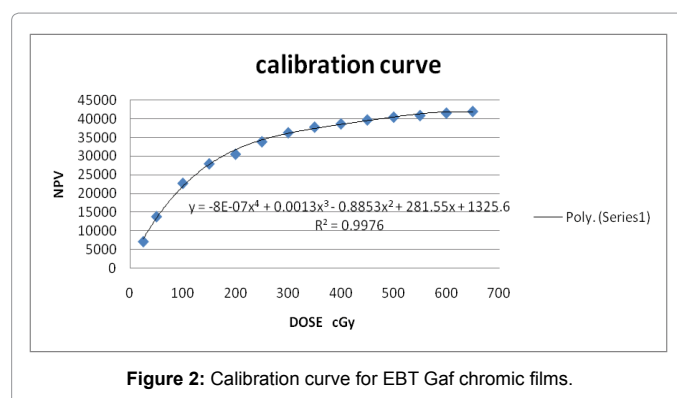


Figure 2: Calibration curve for EBT Gaf chromic films.

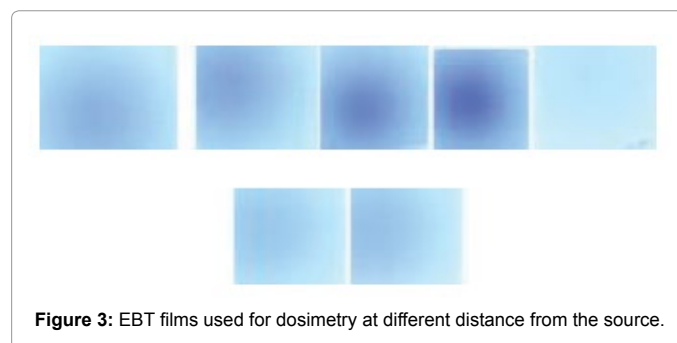


Figure 3: EBT films used for dosimetry at different distance from the source.



Figure 4: Phantom for Monte Carlo validation.

greater than 4 cm, as the modeled source core is not a line, but it was cylindrical in-shape. Corresponding is dose contours were calculated for the single ^{192}Ir source situated in the center of the 15 cm radius water equivalent phantom and compared with the result of experimental examination of phantom validation. A general consideration of the dose results shows an excellent agreement (better than 2%) between the MC code and the measured isodose contours.

Inhomogeneity results

X-rays were simulated for the transport of photons, Rayleigh scattering, Compton scattering, photoelectric absorption and fluorescent emission of characteristic. Dose distributions surrounding the source are scored in a 2D mesh of cubic voxels located on a plane defined by the source axis (z-axis) and the transverse axis. MC-calculated doses in the inhomogeneous patient-equivalent geometry are presented in the form of isodose contours normalized to the reference dose, in the transversal plane at $r=1$ cm from the source. The ratios of doses obtained under heterogeneous conditions to doses in homogenous soft tissue conditions were determined using the MC simulation and film dosimetry measurements. In This work in homogeneities were slab with different thickness size. Results are presented in terms of heterogeneity correction factors (HCFs) defined as the ratio of dose to a point with the inhomogeneity in place divided by the dose to the same point with no inhomogeneity. In order to outline the effect of interference of the inhomogeneity in a water medium, MC simulations were performed first in an unbounded and homogeneous water phantom; then in the same phantom containing cortical bone and lung as inhomogeneities. In previous work a 15% overestimation and 13% underestimation by TPS have been experimentally reported for ^{192}Ir brachytherapy which were contributed to the different density and atomic number of inhomogeneities (lung and bone) and also changing of scatter [17]. Selection of slab shaped inhomogeneities and the corresponding symmetry of the simulation geometry were due to achieved facilitates and accuracy to define scoring x, y, z planes in a grid of $2\text{ mm} \times 2\text{ mm} \times 2\text{ mm}$. HCFs just after a short distance behind the heterogeneities interlayer reached to the maximum about 1.03 and 1.02 for the lung (Figure 5), and the minimum about 0.97 and 0.96 for the bone interlayer (Figure 6). For the thicker interlayer (lung and bone interlayer thickness set to 0.6 cm), the tissue heterogeneity shows a significant effect on the dose distribution under the both heterogeneity conditions. For the lung interlayer, when the interlayer thickness increases from 0.6 cm to 2 cm, the dose ratio reaches the maximum about 1.03 and 1.02 from 1.07 and 1.08 (Figure 7); while for the bone

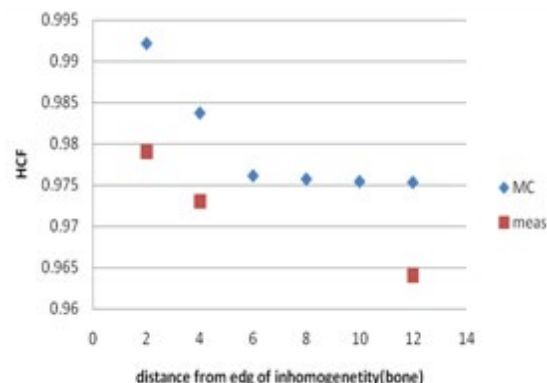


Figure 5: Diagram of correction factor with 6 mm thickness of bone inhomogeneity at 6 mm distance from the source.

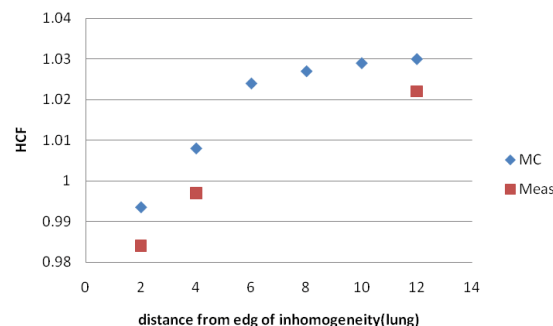


Figure 6: Diagram of correction factor with 6 mm thickness of lung inhomogeneity at 6 mm distance from the source.

interlayer, the minimum dose ratio decreases from 0.97 and 0.96 to 0.92 and 0.91 as the thickness of the interlayer increases from 0.6 cm to 2 cm (Figure 8). TPS fails to predict an increase of scattered, and thus the total dose for bone inhomogeneities relative to corresponding point in homogeneous water geometry as well as the inverse effect of a slight decrease of scatter, and thus the total dose just before the lung inhomogeneities relative to corresponding point in homogeneous water geometry.

In the both interlayer models, the presence of the heterogeneity interlayer has a remarkable effect on the dose distribution for an orthovoltage energy source implant. Comparing with the homogeneous media condition, it is noted that for the lung interlayer models, the dose distribution has an increasing trend within the interlayer. This could be due to the influence of the interlayer on the original of the radiation field under the homogeneous condition, lower effective atomic numbers and density in the lung than those in soft tissue. Therefore, the penetrating ability of photons in lung is higher than that in soft tissue and the dose ratios rise within the interlayer. Hence, by considering that the effective atomic number and density of air are lower than those of lung, with replacing air instead of lung, as inhomogeneity layer, higher dose ratios were observed.

This confirms the conclusion of previous works implying that heterogeneity is affected by the effective atomic number and density, and this factor increases with decreasing effective atomic number of

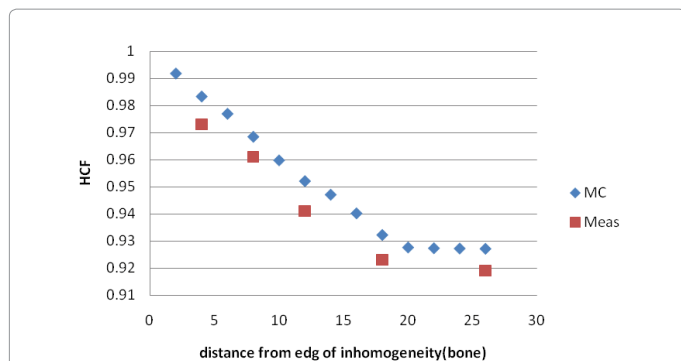


Figure 7: Diagram of correction factor with 20 mm thickness of bone inhomogeneity at 6 mm distance from the source.

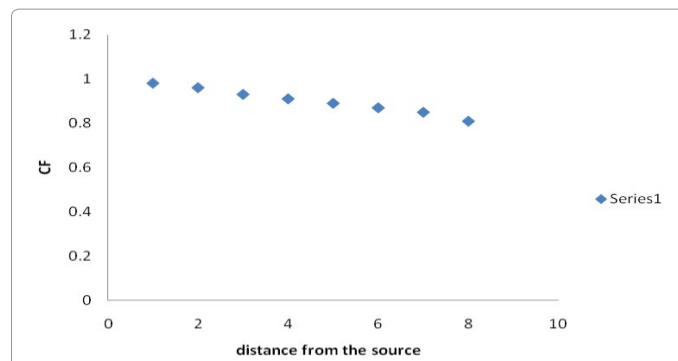


Figure 9: Diagram of dose correction factor for source position using Monte Carlo simulation.

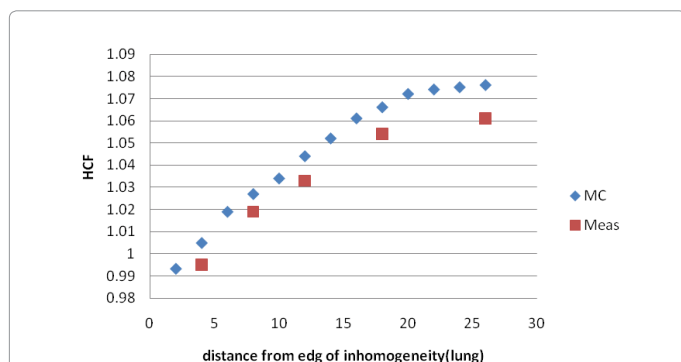


Figure 8: Diagram of correction factor with 20 mm thickness of lung inhomogeneity at 6 mm distance from the source.

the heterogeneity [17,32]. In contrast, the effective atomic number and density of bone is much higher than those of the lung and soft tissue; thus, the penetrating ability of photons in bone is lower than that in lung and soft tissue. As a result, in contrast to the lung interlayer models, the dose ratios show a descending trend in the bone interlayer. Additionally, this calculation shows that the magnitude of the heterogeneity effect does not reach the maximum right after the heterogeneity interlayer; where it reaches the maximum after a relative distance from the heterogeneity interlayer. This phenomenon is due to the contribution of the scattered dose in calculations. The EBT film dosimetry measurements have shown fairly good agreement with the MC calculation results. At the points before the inhomogeneity's, the TPS fails to predict a slight increase of scattered dose (and thus the total dose) just before the bone inhomogeneity's relative to corresponding results in the homogeneous water geometry; like the inverse effect of a slight decrease of scattered dose (and thus the total dose) just before the lung inhomogeneities relative to the corresponding results in a homogeneous water geometry. These observed discrepancies are due to the fact that the TPS does not capable of accounting the minor differences in the backscattered radiation. However, comparison between the MC and experiments with TPS results reveals that the presence of the surrounding inhomogeneities does not affect on the dose distribution in the planning target volume (PTV). This is due to the predominance of the primary dose component at distances close to the source where the PTV is situated (Figure 9).

In this work we also considered the effect of phantom boundaries in dose distribution around the source. It is evident that as bounded phantom radius increases, the lack of backscatter relative to the unbounded phantom decrease. Figures reveal that close to the phantom edge TPS dose results that resemble MC calculations overestimate total dose maximum by 96% that reaches to 82% for greater distance from the source. These results for film were 92% and 79% respectively. A general inspection of the dose at different points of the phantom reveals that as the source moves toward the edge of the phantom, TPS overestimates dose and increases dose overestimation at points lying far from the source in the innermost side of the phantom. At points lying in the proximal side of the phantom surface it can be seen that although TPS and MC results are not in close agreement, for points lying far from the source, TPS results reveal more dose overestimation. This TPS dose overestimation effect can be explained by the increasing lack of backscatter as one move closer to the phantom edge, combined; however, considering the fact that for the ^{192}Ir energies, scatter radiation builds up gradually and contributes for the better part of total dose beyond 6 cm from a source.

Conclusion

In this study the effects of tissue heterogeneity and phantom dimension on dose distribution for ^{192}Ir HDR source in brachytherapy treatment planning system (TPS) using Monte Carlo (MC) technique and film dosimetric measurements have been investigated. Comparison between MCNP4C and film dosimetric measurements with corresponding Felexitron version 14.2.4 dose results in an inhomogeneous patient equivalent phantom geometry revealed that the dose in the planning treatment volume (PTV) is not altered by the presence of the surrounding inhomogeneities and TPS for PTV is credible. Results also shown that all percentage isodose contours greater than 60% (near the source) are not affected by the factors that not considered by the TPS namely the finite patient dimensions and the presence of the lung, bone and other inhomogeneities; however, TPS calculations were underestimated dose by up to 8.2% in the lung specially relatively away from the implant and overestimated dose by up to 9% in the bone. These values were also confirmed the corresponding dose-volume histogram analysis results. The magnitude of correction factors is significantly dependent on the distance and thickness as well as the condition of partial or full heterogeneity. MC calculations and film measurements are in good agreement with each other and agree with the available published data. Thus, TPSs currently in use for clinical brachytherapy cannot consider the effect of tissue heterogeneity on dose distribution. TPS sellers must provide

heterogeneity correction factor for all commonly used brachytherapy TPSs. Comparing MC calculations and film measurement resulted in the actual inhomogeneous geometries shows that for clinical application, MC calculation has an excellent accuracy in determining dose in geometries containing any of tissue type inhomogeneity (bone, lung, etc.) regardless of its thickness or position relative to the source but is very time consuming method.

Acknowledgement

The authors would like to thank Dr. Mahmoud Allah Verdy, may God bless him; Dr. Abbas Takavar, and Dr. Ramin Jaberri for their valuable consults and technical assistances.

References

- Vratislav S, Potter R, Kovács G, Block T (2010) Practical handbook of brachytherapy. Bremen: UNI-MED Verlag, Germany.
- de Brabandere M, Mousa AG, Nulens A, Swinnen A, Limbergen EV (2008) Potential of dose optimisation in MRI-based PDR brachytherapy of cervix carcinoma. *Radiother Oncol* 88: 217-226.
- Khan FM, Stathakis S (2010) The physics of radiation therapy. *Med Phys* 37: 1374.
- Rivard MJ, Butler WM, DeWerd LA, Huq MS, Ibbott GS, et al. (2007) Supplement to the 2004 update of the AAPM Task Group No. 43 Report. *Med Phys* 34: 2187-2205.
- Perez-Calatayud J, Ballester F, Das RK, DeWerd LA, Ibbott GS, et al. (2012) Dose calculation for photon-emitting brachytherapy sources with average energy higher than 50 keV: report of the AAPM and ESTRO. *Med Phys* 39: 2904-2929.
- Zourari K, Pantelis E, Moutsatsos A, Petrokokkinos L, Karaiskos P, et al. (2010) Dosimetric accuracy of a deterministic radiation transport based 192Ir brachytherapy treatment planning system. Part I: Single sources and bounded homogeneous geometries. *Med Phys* 37: 649-661.
- Emily P, Verhaegen F (2009) Development of a scatter correction technique and its application to HDR 192Ir multicatheter breast brachytherapy. *Med Phys* 36: 3703-3713.
- Chica U, Anguiano M, Lallena AM (2009) Benchmark of PENELOPE for low and medium energy X-rays. *Phy Med* 25: 51-57.
- Amoush A, Luckstead M, Lamba M, Elson H, Kassing W (2013) A comparison of HDR near source dosimetry using a treatment planning system, Monte Carlo simulation, and radiochromic film. *Med Dosim* 38: 160-164.
- Sina S, Faghihi R, Meigooni AS (2015) A New Approach for Heterogeneity Corrections for Cs-137 Brachytherapy Sources. *J Biomed Phys Eng* 5: 53-58.
- Dolan J, Lia Z, Williamson JF (2006) Monte Carlo and experimental dosimetry of an 125I brachytherapy seed. *Med Phys* 33: 4675-4684.
- Allahverdi M, Sarkhosh M, Aghili M, Jaberri R, Adelnia A, et al. (2012) Evaluation of treatment planning system of brachytherapy according to dose to the rectum delivered. *Radiat Prot Dosimetry* 150: 312-315.
- Thomson RM, Taylor REP, Rogers DWO (2008) Monte Carlo dosimetry for 125I and 103Pd eye plaque brachytherapy. *Med Phys* 35: 5530-5543.
- Mowlavi AA, Cupardo F, Severgnini M (2006) Monte Carlo and experimental relative dose determination for an Iridium-192 source in water phantom. *Ir J Radiat Res* 6: 37-42.
- Furutani S, Saze T, Ikushima H, Oita M, Ozaki K, et al. (2006) Quality assurance of I-125 seeds for prostate brachytherapy using an imaging plate. *Int J Radiat Oncol Biol Phys* 66: 603-609.
- Bernadette H, Martišiková M, Jäkel O (2010) Technical note: homogeneity of Gafchromic® EBT2 film. *Med Phys* 37: 1753-1756.
- Anagnostopoulos G, Baltas D, Pantelis E, Papagiannis P, Sakelliou L (2004) The effect of patient inhomogeneities in oesophageal 192Ir HDR brachytherapy: a Monte Carlo and analytical dosimetry study. *Phys Med Biol* 49: 2675-2685.
- Chandola R, Tiwari S, Kowar M, Choudhary V (2010) Effect of inhomogeneities and source position on dose distribution of nucletron high dose rate Ir-192 brachytherapy source by Monte Carlo simulation. *J Cancer Res Ther* 6: 54-57.
- Barlanka R, Lakshminarayana S (2012) Determination of the tissue inhomogeneity correction in high dose rate Brachytherapy for Iridium-192 source. *J Med Phys* 37: 27-31.
- Nedaie HA, Mosleh-Shirazi MA, Allahverdi M (2013) Monte Carlo N Particle Code - Dose Distribution of Clinical Electron Beams in Inhomogeneous Phantoms. *J Med Phys* 38: 15-21.
- Solomon CJ, Sood A, Booth TE, Shultis JK (2014) A Priori Deterministic Computational-Cost Optimization of Weight-Dependent Variance-Reduction Parameters for Monte Carlo Neutral-Particle Transport. *Nucl Sci Eng* 176: 1-36.
- Taleei R, Shahriari M (2009) Monte Carlo simulation of X-ray spectra and evaluation of filter effect using MCNP4C and FLUKA code. *App Radiat Isot* 67: 266-271.
- X-5 Monte Carlo Team (2003) MCNP – A General Monte Carlo N-Particle Transport Code, Version 5. Volume I: Overview and Theory. Los Alamos National Laboratory, University of California, USA.
- Emily P, Verhaegen F (2009) A CT-based analytical dose calculation method for HDR 192Ir brachytherapy. *Med Phys* 36: 3982-3994.
- Wai P, Adamovics J, Krstajic N, Ismail A, Nisbet A, et al. (2009) Dosimetry of the microSelectron-HDR Ir-192 source using PRESAGE™ and optical CT. *Appl Radiat Isot* 67: 419-422.
- Koulouklidis AD, Cohen S, Kalef-Ezra J (2013) Thermochromic phase-transitions of GafChromic films studied by z-scan and temperature-dependent absorbance measurements. *Med Phys* 40: 112701.
- Meira-Belo LC, Rodrigues EJ, Grynberg SE (2013) Methodology for characterizing seeds under development for brachytherapy by means of radiochromic and photographic films. *Appl Radiat Isot* 74: 26-30.
- Andres C, DelCastillo A, Tortosa R, Alonso D, Barquero R, et al. (2010) A comprehensive study of the Gafchromic EBT2 radiochromic film. A comparison with EBT. *Med Phys* 37: 6271-6278.
- Soares CG (2006) Radiochromic film dosimetry. *Radiat Meas* 41: S100-S116.
- Martišiková M, Ackermann B, Jäkel O (2008) Analysis of uncertainties in Gafchromic® EBT film dosimetry of photon beams. *Phys Med Biol* 53: 7013.
- Menegotti L, Delana A, Martignano A (2008) Radiochromic film dosimetry with flatbed scanners: a fast and accurate method for dose calibration and uniformity correction with single film exposure. *Med Phys* 35: 3078-3085.
- Richley L, John AC, Coomber H, Fletcher S (2010) Evaluation and optimization of the new EBT2 radiochromic film dosimetry system for patient dose verification in radiotherapy. *Phys Med Biol* 55: 2601.